Journal of Macromolecular Science, Part A
Publication details, including instructions for authors and subscription information:
http://www.informaworld.com/smpp/title~content=t713597274

Synthesis and Characterization of Functional Gradient Copolymers of 2-Hydroxyethyl Methacrylate and *tert*-Butyl Acrylate by Atom Transfer Radical Polymerization

Juan He[ab]; Yufeng Wang[ac]; Qunfang Lin[a]; Ligen Chen[a]; Xiaodong Zhou[b]
[a] School of Materials Science and Engineering, East China University of Science and Technology, Shanghai, P.R. China [b] State Key Laboratory of Chemical Engineering, East China University of Science and Technology, Shanghai, P.R. China [c] Shanghai Zhongyuan Chemical Company Limited, Shanghai, P.R. China

To cite this Article He, Juan , Wang, Yufeng , Lin, Qunfang , Chen, Ligen and Zhou, Xiaodong(2009) 'Synthesis and Characterization of Functional Gradient Copolymers of 2-Hydroxyethyl Methacrylate and *tert*-Butyl Acrylate by Atom Transfer Radical Polymerization', Journal of Macromolecular Science, Part A, 46: 4, 405 — 411
To link to this Article: DOI: 10.1080/10601320902728702
URL: http://dx.doi.org/10.1080/10601320902728702

Journal of Macromolecular Science®, Part A: Pure and Applied Chemistry (2009) **46**, 405–411

ISSN: 1060-1325 print / 1520-5738 online
DOI: 10.1080/10601320902728702

Taylor & Francis
Taylor & Francis Group

Synthesis and Characterization of Functional Gradient Copolymers of 2-Hydroxyethyl Methacrylate and *tert*-Butyl Acrylate by Atom Transfer Radical Polymerization

JUAN HE[1,2], YUFENG WANG[1,3], QUNFANG LIN[1], LIGEN CHEN[1] and XIAODONG ZHOU[2]

[1]*School of Materials Science and Engineering, East China University of Science and Technology, Shanghai 200237, P.R. China*
[2]*State Key Laboratory of Chemical Engineering, East China University of Science and Technology, Shanghai 200237, P.R. China*
[3]*Shanghai Zhongyuan Chemical Company Limited, Shanghai 200431, P.R. China*

Received October 2008, Accepted November 2008

Functional spontaneous gradient copolymers of 2-hydroxyethyl methacrylate (HEMA) and *tert*-butyl acrylate (*t*BA) were synthesized by atom transfer radical polymerization (ATRP) in cyclohexanone at 50°C. The copolymers were characterized by nuclear magnetic resonance spectroscopy (^{1}H-NMR) and gel permeation chromatograph (GPC). Comonomer conversions were determined by gas chromatograph (GC) and the kinetic behavior for HEMA/*t*BA copolymerization was analyzed, indicating that the copolymerization proceeds in a controlled way. The monomer reactivity ratios $r_{HEMA} = 4.497$ and $r_{tBA} = 0.212$ were estimated using an extended Kelen-Tüdos method from copolymer composition data. Atomic force microscopy (AFM) images demonstrated the changes of surface morphology of poly(HEMA-*grad*-*t*BA) polymerized for different times and the changes were correlated to the composition of the copolymers.

Keywords: atom transfer radical polymerization, 2-hydroxyethyl methacrylate, *tert*-butyl acrylate, gradient copolymers

1 Introduction

Since it was first proposed in 1996 (1), gradient copolymers as a novel class of materials have recently been receiving much attention (2, 3). The structure of gradient copolymers is characterized by a gradual change in composition along the entire copolymer chain backbone. In contrast with block copolymers, where the composition changes abruptly at the block junction point, and random copolymers where there is no statistical change in composition along the copolymer chain, gradient copolymers are in between. Therefore, gradient copolymers are expected to possess not only the similar properties as block or random copolymers, but also some newer and more specialized qualities that they do not have. In some recent reports, gradient copolymers were found to exhibit nanoheterogeneous morphologies, with single, broad, tunable glass transitions temperatures and would be ideal candidates for damping applications (4, 5). Because gradient copolymers may possess significantly larger critical micelle concentration (cmc) values in homopolymer than those associated with block copolymers (6), they are more effective than block copolymers when used as compatibilizers of immiscible polymer blends (7, 8). More recently, an interesting phenomenon discovered by Okabe et al. (9) was that the micellization of gradient copolymer in aqueous solution was continuous and the micelle sizes can gradually change with increasing temperature. As yet, the preparation and application of gradient copolymers have not been thoroughly explored.

Two methods are generally used to synthesize gradient copolymers. The first is based on the differences in the reactivity ratios of the comonomers and the concentrations of comonomers in the feed, using batch copolymerization to produce spontaneous gradient copolymers. The second depends on the addition of one of the comonomers to the copolymerization mixture during the reaction process, using semi-batch copolymerization to obtain "forced" gradient copolymers (2). Many gradient copolymers have been prepared using the first method for its convenient setups. In order to obtain a gradient copolymer with similar gradient in composition along each single polymer chain, there should be simultaneous initiation and uniform growth of all chains. In addition, facile cross-propagation is

Address correspondence to: Xiaodong Zhou, State Key Laboratory of Chemical Engineering, East China University of Science and Technology, Shanghai 200237, China. Tel: 86-021-64253757; Fax: 86-021-64253757. E-mail: xdzhou@ecust.edu.cn

required. Neither regular radical polymerization nor living ionic polymerization processes fulfill these requirements. However, the new techniques of controlled/living radical polymerization (CPR) made it possible to prepare well-defined gradient copolymers (2, 10).

Atom transfer polymerization (ATRP) is one of the most powerful and versatile methods in controlled/living radical polymerization. Because of the radical nature of ATRP, a wide range of functional monomers can be (co)polymerized in a controlled fashion, resulting in polymers with pendant functional groups (11, 12). Thus, if functionalized comonomers are properly selected, numerous functional gradient copolymers will be synthesized via ATRP with potential advantages for more novel materials. By the reaction of functional groups in the copolymer, various kinds of polymeric architecture can be formed. There are some cases of functional gradient copolymers. For instance, Matyjaszewski and co-workers (13) first used 2-(trimethylsilyloxy)ethyl acrylate (HEA-TMS) and methyl methacrylate (MMA) to produce spontaneous gradient copolymers, and then transformed to macroinitiators for the sake of preparing molecular brushes with gradient in grafting density. Also, another spontaneous gradient copolymer with a pendant, crosslinkable functional group was prepared by París and De La Fuente (14), using allyl methacrylate and n-BA as comonomers.

In this work, we report the statistical copolymerization of 2-hydroxyethyl methacrylate (HEMA) and *tert*-butyl acrylate (*t*BA) via ATRP in cyclohexanone. It is well known that HEMA, which owns a hydroxyl group in molecular structure, is an important functional monomer to manufacture various materials like contact lenses (15), drug delivery (16), biocompatibilization (17). While *t*BA is recently most used in the preparation of amphiphilic block copolymers since the *tert*-butyl ester groups can be easily transformed into carbonic acid groups by acidic hydrolysis. The copolymer of HEMA and *t*BA may be of potential application considering that hydroxyl groups or *tert*-butyl ester groups can react with many other chemicals obtaining novel materials. The present work describes the kinetic features of ATRP of HEMA and *t*BA. The synthesized copolymers were characterized by gel permeation chromatograph (GPC) and nuclear magnetic resonance spectroscopy (^{1}H-NMR). The monomer reactivity ratios determined helps to indicate the possibility of forming spontaneous gradient copolymers. In addition, AFM images of copolymers that reacted for different time were depicted primarily. Further study will focus on the self-assembly of the gradient copolymer derived from poly(HEMA-*grad*-*t*BA).

2 Experimental

2.1 Materials and Reagents

HEMA, (98%, Acros) was purified by passing the neat liquids through a column filled with neutral alumina to remove the inhibitor, eluted with 30/70 benzene/ethyl acetate, and distilling under reduced pressure (18). *tert*-Butyl acrylate (*t*BA, Aldrich, 98%) was washed with 5% aqueous NaOH solution, dried over anhydrous $CaCl_2$, vacuum distilled and stored in the refrigerator. CuCl (AR, Shanghai No. 1 Chemical Plant) was purified by stirring overnight in acetic acid. After filtration it was washed with ethanol, ether, and then dried. Cyclohexanone (AR, Shanghai No. 1 Chemical Plant) was distilled before use. ethyl 2-bromoisobutyrate (EB*i*B, Aldrich, 98%), and *N*, *N*,*N*′,*N*″,*N*′ ″-pentamethyldiethylenetriamine (PMDETA, Aldrich, 99%) were used as received.

2.2 Synthesis of Poly(HEMA-grad-tBA)

In a typical experiment, PMDETA (0.413 g, 2.4 mmol), *t*BA (22.958 g, 0.179 mol), and HEMA (23.308 g, 0.179 mol) were added into a 100 mL Schlenk flask, and the resulting solution was degassed by three freeze-pump-thaw cycles. Then, CuCl (0.119 g, 1.2 mmol) was added under stirring, followed by immersing the Schlenk flask in a thermostated oil bath at 50°C. After 3 min, the initiator EB*i*B (174.9 μL; 1.2 mmol) was injected into the mixture via a syringe, and an initial kinetic sample was taken. During polymerization, samples were removed periodically to determine conversion by GC and molecular weight by GPC. After completion of the reaction, the crude product was diluted in acetone, and filtered through a neutral alumina column to remove the copper catalyst. Next, the solvent was removed, and the polymer was dried under vacuum to a constant weight.

2.3 Measurements

Comonomer conversion was determined using an Agilent Technologies 6850 Series II Network GC system equipped with a poly (dimethylsiloxane) capillary column (12 m × 200 μm × 0.25 μm). GC was performed using H_2 as eluent at a flow rate of 1.5 mL/min and employing a temperature ramp rate of 10°C/min. The temperature of flame ionization detector was 300°C with a H_2 flow rate of 40 mL/min. 1,2,4-trimethoxybenzene (1/1 v/v to HEMA) was added to the polymerization medium as an internal GC standard. GC samples were diluted with acetone prior to characterization. ^{1}H-NMR spectrum was recorded on a Bruker Avance spectrometer at 400 MHz. Deuterated acetone was used as a solvent, and tetramethylsilane served as an internal standard. Multi-detector gel permeation chromatograph (GPC) equipment is composed of a Waters 515 HPLC pump, three MZ-Gel plus 10E6Å, 10E5Å and 10E3Å columns connected in series and an Optilab Rex refractive index detector (Wyatt Technology Corp.) combine with a multi-angle laser scattering detector (DAWN-HELEOS, Wyatt Technology Corp.), which can provide an absolute molecular weight of polymers. The

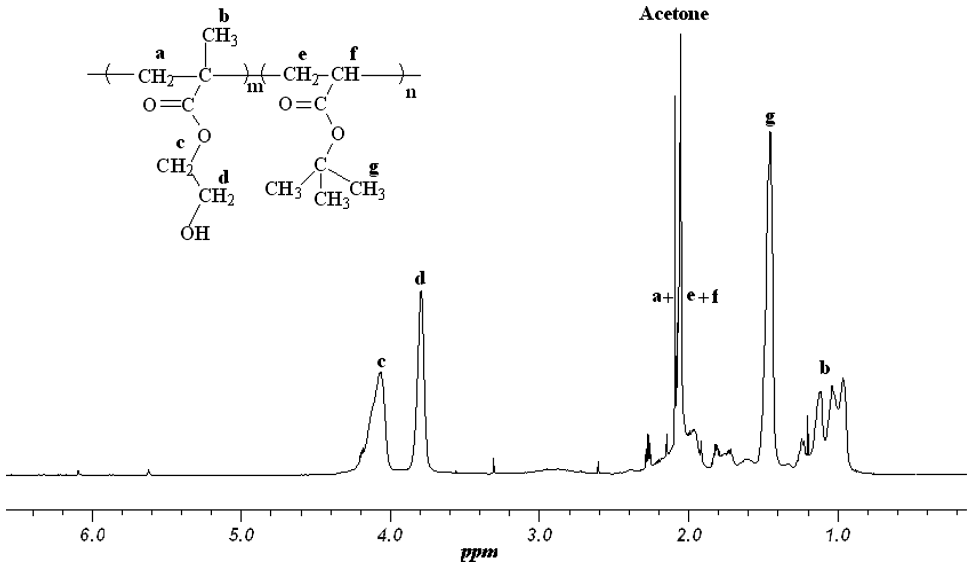

Fig. 1. ^{1}H-NMR spectrum of Poly(HEMA-*grad*-*t*BA)(40/60) in d_6-acetone.

eluent was THF with a flow rate of 1 mL/min. Atomic force microscopy (AFM) was performed using a Multimode scanning probe microscope (NanoScope III a MultiMode AFM Digital Instruments) in tapping mode with a silicon tip. Ultrathin films were prepared by spin-coating dilute copolymer solutions in acetone onto freshly cleaved mica at room temperature. By using the same solution concentration (0.5 wt%) and the same rotation speed (4000 rpm for 30 s), a series of ultrathin films with uniform thickness can be obtained.

3 Results and Discussion

3.1 Synthesis of Gradient Copolymers

Since it is well-known that better molecular weight control was observed by using the halogen-exchange technique (19, 20), we employed CuCl/PMDETA as the catalyst system and EB*i*B as the initiator in this copolymerization. Furthermore, such mixed halide systems are especially effective for the polymerization of monomers with high propagation constants, such as HEMA (21). Previous research on (co)polymerization of HEMA via ATRP was mostly carried out in protic solvents. However, copper-mediated ATRP in protic solvents has the characterization of inefficient deactivation and leads to poorly controlled polymerization (22). Moreover, the degree of polymerization of the HEMA homopolymer prepared by aqueous ATRP is readily controlled in the range of 10–75 (23), which becomes the limitation for exploiting more HEMA-based materials. Herein, we choose cyclohexanone, in which many polymers and ATRP catalysts are well dissolved, as the solvent for copolymerization of HEMA and *t*BA.

A series of copolymers were prepared by ATRP of HEMA and *t*BA with various feed composition, using EB*i*B as initiator and CuCl/PMDETA as catalyst at 50°C. The molar ratio of HEMA and *t*BA can be determined from ^{1}H-NMR.

Figure 1 shows the ^{1}H-NMR spectrum of the copolymer of poly(HEMA-*grad*-*t*BA) (molar feed ratio is 40/60) dissolved in *d*6-acetone. The peak (d) at 3.80 ppm is assigned to the methylene protons adjacent to the hydroxy group in HEMA monomer unit while the peak (g) at 1.45 ppm is due to the protons in *tert*-butyl group. The broad resonance signals between 1.6 and 2.4 ppm are attributed to the methylene protons and the methine protons existing in the repeat unit of the main chain. No signals between 7.5 and 5.5 ppm are observed indicating the absence of double bonds. From the peak intensity of (d) and (g), we accurately calculated the molar fraction of monomer units incorporated into the copolymer chains. The results for obtained copolymers are presented in Table 1.

Table 1. Experimental data for various copolymers of HEMA/*t*BA prepared by ATRP

Sample[a]	*molar feed ratio (HEMA/tBA)*	f^b_{HEMA}	F^c_{HEMA}	*Conversion (%)*
1	70/30	0.70	0.925	36.2
2	55/45	0.55	0.839	42.2
3	40/60	0.40	0.726	31.9
4	25/75	0.25	0.610	25.5
5	10/90	0.10	0.340	11.2

[a]Reaction conditions: $(HEMA/tBA)_0$: (EBiB): (CuCl): (PMDETA) =1 00:1:1:2; 50°C; 1:1 by vol monomer/cyclohexanone.
[b]f_{HEMA} is the mole fraction of HEMA in the feed.
[c]F_{HEMA} is the mole fraction of HEMA in the copolymer determined by ^{1}H-NMR.

3.2 Determination of Monomer Reactivity Ratios

Based on the composition of copolymers determined by ^{1}H-NMR (as seen in Table 1), the reactivity ratios of HEMA/*t*BA monomer pair can be estimated. There are some existing procedures for calculating reactivity ratios, such as Fineman-Ross (24), Mayo-Lewis (25) and Kelen-Tüdös (26) methods. But all these calculations are based on the differential copolymerization equation, thus, the copolymerization must be controlled at sufficiently low conversion (usually less than 10%). The extended Kelen-Tüdös method (27), which can be applied to medium-high conversion without significant systematic error, is used to determine the reactivity ratios. Reactivity ratios r_{HEMA} and r_{tBA} of the copolymerization of HEMA and *t*BA by ATRP are 4.497 and 0.212, respectively.

A relatively large difference was found in the reactivity ratios of the two monomers, as expected, since the HEMA/*t*BA copolymerization is a methacrylate/acrylate system. The high value of r_{HEMA} indicates that the probability of HEMA entering the copolymer chain is much higher than that of *t*BA. In such a system, where $r_{HEMA} \gg r_{tBA}$, a spontaneous gradient copolymer should to be formed (28–31).

The plot of mole fraction of HEMA (f_{HEMA}) in the feed vs. that in the copolymer (F_{HEMA}) is shown in Figure 2. The curve is above the diagonal of the diagram, which indicates that the composition of HEMA in the copolymer is always higher than that in the feed. This can be explained from the reactivity ratios of HEMA/*t*BA monomer pair. In this case, the value of r_{HEMA} is greater than 1 and the value of r_{tBA} is less than 1, suggesting that the polymeric radical reacts faster with HEMA than with *t*BA. Therefore, the probability of HEMA entering into the copolymer chain is higher compared to *t*BA. Furthermore, as to a typical batch copolymerization, copolymers formed at the beginning of the reaction are richer in HEMA. As the copolymerization proceeds, the concentration of residual HEMA monomers decreases rapidly, while that of *t*BA remains at a relatively high level, leading to a faster rate of *t*BA propagating into the copolymer chain. Thus, the final copolymers obtained, namely gradient copolymers, have a composition which changes gradually from predominant sequences of HEMA to *t*BA as a function of the copolymer chain length.

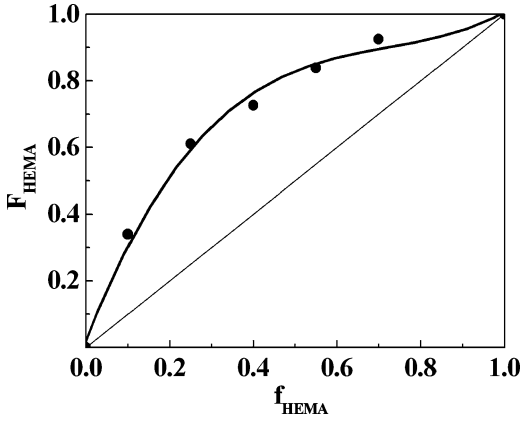

Fig. 2. Relationship between HEMA in the feed (f_{HEMA}) and HEMA incorporated into the copolymers (F_{HEMA}).

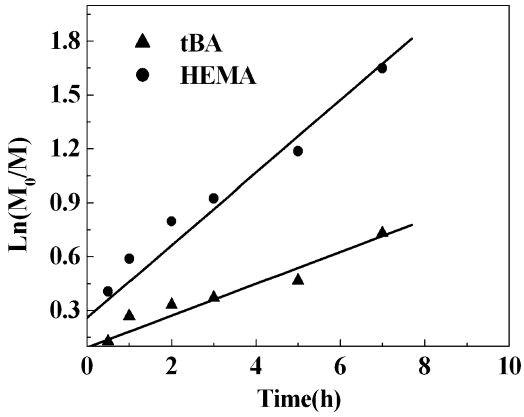

Fig. 3. Kinetic plots for the copolymerization of HEMA/*t*BA by ATRP in cyclohexanone at 50°C.

3.3 Gradient Copolymerization Kinetics

HEMA/*t*BA monomer pair was chosen for the preparation of spontaneous gradient copolymers due to the relatively large differences in the monomer reactivity ratios. In the one-pot copolymerization, a 1:1 molar feed ratio of HEMA and *t*BA was selected. Figure 3 demonstrates the kinetic plots of copolymerization of HEMA and *t*BA. The linearity of the plot of ln($[M]_0/[M]$) vs. time indicates the copolymerization follows first-order kinetics with respect to monomer concentration. It also shows that HEMA is consumed at a faster rate than *t*BA and after 7 h, the conversion of HEMA and *t*BA reaches 78% and 50%, respectively, yielding a gradient copolymer.

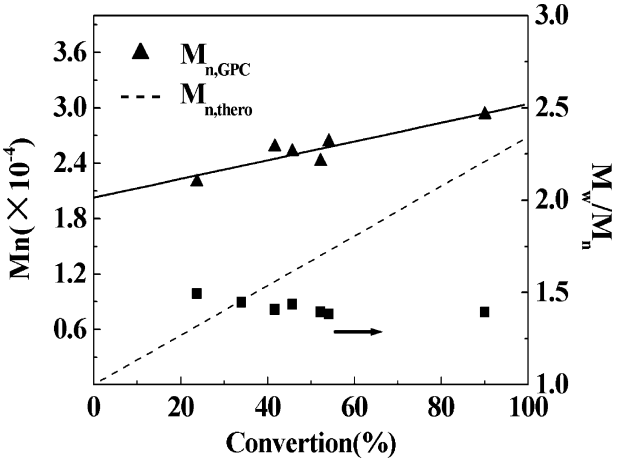

Fig. 4. Molecular weight and polydispersity data for ATRP of HEMA with *t*BA.

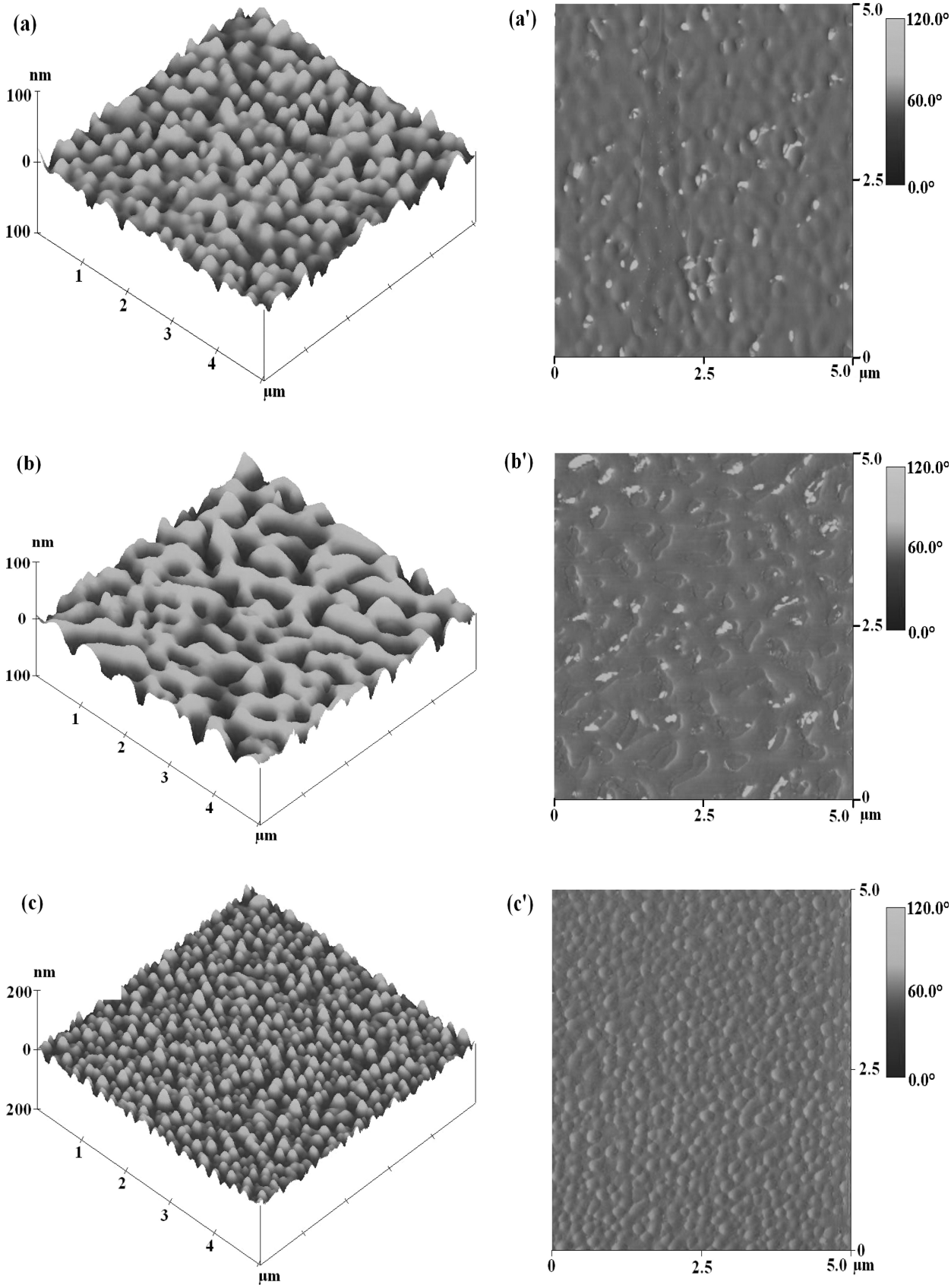

Fig. 5. Tapping mode AFM three-dimensional height (left) and phase (right) images of poly(HEMA-*grad*-*t*BA) removed from the reaction at (a) 0.5 h, (b) 3 h, and (c) 7 h .

The dependence of Mn on monomer conversion is illustrated in Figure 4. Although a linear increase of Mn vs. monomer conversion is depicted, there is a significant discrepancy between the GPC data and the theory molecular weights. A similar phenomenon has been previously reported by Beers et al. (18) that the molecular weight of PHEMA homopolymers determined by GPC is nearly twice the actual values. This is presumably due to the discrepancy calibration errors in the GPC analysis. However, our research possesses something different from theirs. On one hand, we measured the molecular weight of copolymers using a multi-detectors GPC equipped with a DAWN HELEOS static laser scattering detector and an Optilab Rex refractive index detector, which provides an absolute molecular weight and needs no polymer standards. Thus, we consider that the discrepancy may mainly be caused by intermolecular aggregates among polymers, for there are quantities of hydroxyl groups in PHEMA segments to form hydrogen bonding. On the other hand, the polymer we studied is a gradient copolymer containing PHEMA moieties. Unlike the homopolymers of PHEMA in Beers' work, the experimental Mn values of copolymers in our study are not always double the theoretical ones, but 2 or 3 times as large as theoretical values first, and then gradually closer to it. Considering that the hydrophobic P*t*BA segments in copolymers would weaken the effect of hydrogen bonding, the gradual closeness of GPC data to theoretical data indicates a gradual increase in the incorporation of *t*BA into the copolymer as the reaction progresses, and ultimately forms a *t*BA-rich chain end. Furthermore, the distribution of molecular weight gradually became narrow for the same reason. These features may illustrate the formation of gradient structure from another point of view.

3.4 AFM Analysis

Tapping mode atomic force microscopy (TM-AFM) was used to study the surface morphology of Poly(HEMA-*grad*-*t*BA) in different compositions. The samples for AFM observation were the same as those for kinetic analysis, which were periodically withdrawn from the reaction. The copolymers polymerized for 0.5, 3 and 7 h were typically selected for contrast.

Figure 5 shows AFM images of the polymer films cast from 0.5% w/w solutions. Different macroscopic phase-separated structures were found by comparing the presented images. The TM-AFM height images show a spherical pattern in both Figures 5(a) and (c), and a worm-like pattern in Figure 5(b). Compared to the height images, the phase images give a better contrast of morphological features due to the distribution of the materials of different module at the film surface: the light domains correspond to soft materials which induce more phase lag of the cantilever, while the dark domains correspond to the hard materials which induce less phase lag (32). Since the segments of PHEMA (Tg = 358K) are relatively harder than that of P*t*BA (Tg = 304K) according to the literature (33), it can be concluded that the darker domains are PHEMA-rich phase and the lighter domains are P*t*BA-rich phase (see Figure 5(a'-c')). When shown in the three-dimensional height images, the PHEMA-rich phase appeared as protuberant parts.

In view of the same conditions that all these films were prepared, the only difference is the copolymer compositions in each sample. So, the changes in AFM images can be correlated with the differences in copolymer compositions which have been determined in kinetic analysis (Figure 3). As shown in Figure 5(a), the features corresponding to PHEMA-rich phase appeared as spherical particles dispersed in a continuous P*t*BA-rich phase, though the mole fraction of PHEMA segments is somewhat larger than that of P*t*BA segments. It appears that acetone is a relatively selective solvent for P*t*BA by comparing the solubility parameters of acetone with PHEMA and P*t*BA ($\delta_{\text{acetone}} = 20.1\ \text{MPa}^{1/2}$, $\delta_{\text{PHEMA}} = 30.1\ \text{MPa}^{1/2}$, $\delta_{\text{PtBA}} = 16.4\ \text{MPa}^{1/2}$) (34, 35). Thus, the segments of PHEMA in different copolymer chains are inclined to assemble and lead to somewhat large particles. In the case of copolymer reacted for 3 h (Figure 5(b)), a wormlike phase of PHEMA is seen due to the overwhelming majority of PHEMA cumulated in polymer chains. While the AFM image of the sample was finally obtained after 7 h, the PHEMA-rich phase presented again as round domains, but the size appears smaller in contrast with those in Figure 5(a). The reason almost certainly is that the increased amount of *t*BA in copolymer chains can hinder the aggregate of PHEMA segments to a certain extent. However, the reliable phase assignment and the detailed mechanism of contrast still require further study, which will be a separate subject of our research and will be reported elsewhere.

4 Conclusions

Functional spontaneous gradient copolymers of HEMA/*t*BA were successfully prepared by ATRP. The copolymerization exhibited all the features of a controlled system. The relatively large difference between the value of r_{HEMA} (4.497) and r_{tBA} (0.212) allowed us to consider that a spontaneous gradient copolymer should be synthesized, with densely HEMA segments incorporated at the beginning of the copolymerization. Furthermore, copolymers drawn at different times showed different surface morphology in tapping mode atomic force microscopy observation which helped to explain the course of gradient copolymerization more visually.

References

1. Pakula, T. and Matyjaszewski, K. (1996) *Macromol Theory Simul.*, 5, 987.
2. Matyjaszewski, K. (2000) *J. Phys. Org. Chem.*, 13, 775–786.

3. Qin, S., Saget, J., Pyun, J. and Matyjasewski, K.(2003) *Macromolecules*, 36, 8969–8977.
4. Mok, M.M. and Torkelson, J.M. (2008) *J. Polym. Sci. Part B: Polym. Phys.,* 46, 48–58.
5. Kim, J., Zhou, H.Y., Nguyen, S.T. and Torkelson, J.M. (2006) *Polymer*, 47, 5799–5809.
6. Shull, K.R. (2002) *Macromolecules*, **35**, 8631–8639.
7. Tao, Y., Kim, J. and Torkelson, J.M. (2006) *Polymer*, 47, 6773–6781.
8. Wong, C.L.H., Kim, J. and Torkelson, J.M. (2007) *Macromolecules*, 40, 5631–5633.
9. Okabe, S., Seno, K. and Shibayama, M. (2006) *Macromolecules*, 39, 1592–1597.
10. Min, K. and Matyjaszewski, K. (2005) *J. Polym. Sci. Part A: Polym. Chem.*, 43, 3616–3622.
11. Coessens, V., Pyun, J. and Matyjaszewski, K. (2000) *Macromol. Rapid. Commun.*, 21, 103.
12. Feng, D., Chandekar, A., Whitten, J.E. and Faust, R. (2007) *J. Macromol. Sci. Part A: Pure and Appl. Chem.*, 44, 1141–1150.
13. Lee, H., Matyjaszewski, K., Yu, S. and Sheiko, S.S. (2005) *Macromolecules*, 38, 8264–8271.
14. Rodrigo, París., José, Luis. and De La Fuente. (2006) *J. Polym. Sci. Part A: Polym. Chem.*, 44, 5304–5315.
15. Wilcox, M.D.P., Harmis, N. and Cowell, B.A. (2001) *Biomaterials*, 22, 3235–3247.
16. Abraham, S., Brahim, S. and Guiseppi-Elie, A. (2005) *Biomaterials*, 26, 4767–4778.
17. Jeyanthi, R. and Rao, K.P. (1990) *Biomaterials*, 11, 238–243.
18. Beers, K.L., Boo, S. and Matyjaszewski, K. (1999) *Macromolecules*, 32, 5772.
19. Matyjaszewski, K., Shipp, D.A. and Wang, J.L. (1998) *Macromolecules*, 31, 6836–6840.
20. Matyjaszewski, K., Shipp, D.A. and McMurtry, G.P. (2000) *J. Polym. Sci., Part A: Polym. Chem*., 38, 2023–2031.
21. Wang, T.L., Liu, Y.Z., Jeng, B.C. and Cai, Y.C. (2005) *J. Polym. Res.*, 12, 67–75.
22. Tsarevsky, N.V. and Matyjaszewski, K. (2004) *Macromolecules*, 37, 9768–9778.
23. Robinson, K.L., Khan, M.A. and Armes, S.P. (2001) *Macromolecules*, 34, 3155.
24. Fineman, M. and Ross, S.D. (1950) *J.Polym. Sic.*, 5, 259–262.
25. Mayo, F.R. and Walling, C. (1950) *Chem. Rev.*, 46, 191–287.
26. Kelen, T. and Tüdös, F. (1975) *J. Macromol. Sci. Chem.*, A9, 1–27.
27. Tüdös, F., Kelen, T. and Földes-Berezsnich, T. (1976) *J. Macromol. Sci. Chem.*, 10, 1513.
28. Matyjaszewski, K. and Ziegler, M. J. (2000) *J. Phys. Org. Chem.*, 13, 775–786.
29. Qin, S., Saget, J. and Matyjaszewski, K. (2003) *Macromolecules*, 36, 8969–8977.
30. Lee, H. and Matyjaszewski, K. (2005) *Macromolecules*, 38, 8264–8271.
31. Min, K. and Matyjaszewski, K. (2005) *J. Polym. Sci. Part A: Polym. Chem.*, 43, 3616–3622.
32. Cong, Y., Li, B.Y. and Han, Y.C. (2005) *Macromolecules*, 38, 9836–9846.
33. Andrews, R.J. and Grulke, E.A. Polymer Hand Book. In Glass Transition Temperatures of Polymers, 4th Ed. Brandrup, J., Immergut, E.H. and Grulke, E.A.(Eds.) John Wiley & Sons Inc.: New York, VI/198-VI/203, 1999.
34. Ray, S. and Ray, S.K. (2006) *J. Membrane Sci.* 270, 73–87.
35. Aydin, S., Erdogan, T. and Sakar, D. (2008) *Eur. Polym. J*., 44**(7)**: 2115–2122.